VILNIUS TECH
Vilnius Gediminas Technical University

Journal of Environmental Engineering and Landscape Management
ISSN 1648–6897 / eISSN 1822-4199
2022 Volume 30 Issue 2: 268–275
https://doi.org/10.3846/jeelm.2022.16743

Special issue on *Sustainable Environmental Processes and Technologies*

SIMULTANEOUS SOLAR PHOTO-DEGRADATION OF PVC-Fe-DOPED ZnO-NANOCOMPOSITE FLAKES AND METHYLENE BLUE DYE IN WATER

Anirban ROY[1*], Sampa CHAKRABARTI[2, 3], Saikat MAITRA[1]

[1]*Maulana Abul Kalam Azad University of Technology, NH-12 (Old NH-34), Simhat, Haringhata, 741249 Nadia, West Bengal, India*
[2]*Department of Chemical Engineering, University of Calcutta, 92 Acharya P. C. Road, 700 009 Kolkata, India*
[3]*Centre for Research in Nanoscience & Nanotechnology, University of Calcutta, JD-2, Sector-III, Salt Lake, 700 098 Kolkata, India*

Received 01 January 2021; accepted 09 June 2021

Highlights

- Simultaneous solar photocatalytic degradation of dye and PVC was studied.
- PVC film impregnated with Fe-ZnO nanoparticles was used as flakes.
- The nanocomposite flakes were found to be self-destructive.
- MB dye also degraded under sunlight along with degradation of the film.
- Both dye and the polymer film followed pseudo-first order kinetics.

Abstract. Simultaneous solar photocatalytic decolorization of Methlene Blue (MB) dye and degradation of polymer nanocomposite film in water has been attempted in the present work. The film immobilized iron (Fe)-doped zinc oxide (ZnO) nanoparticles (NPs) in polyvinyl chloride (PVC) matrix. This reduced the cost of separation of nanoparticles from treated water. Doped NPs were prepared sonochemically using zinc acetylacetonate (0.95 mmol) and ferric acetylacetonate (0.05 mmol) precursors in aqueous ethanol medium. XRD, UV-vis spectroscopy, FESEM and EDX were used for characterizing nanoparticles whereas the film was characterized by SEM. During the process, the film also reduced in weight. Degradation of both the dye and the polymer followed pseudo-first order kinetics. About 28% of the initial concentration of dye and about 5.04% of the initial weight of the PVC-film were decreased in the process after a run time of 3 h 45 minutes.

Keywords: solar photocatalysis, degradation, MB dye, Fe-doped ZnO nanoparticles, PVC-immobilized.

Introduction

Heterogeneous semiconductor photocatalysis was established to be an effective process for degradation of organic contaminants in water (Ai et al., 2011; Chong et al., 2010; Wang et al., 2009). The semiconductors such as TiO_2 or ZnO can be suspended in the wastewater or can be immobilized on a suitable support. Solid materials such as activated carbon (Shi et al., 2008), fiberglass (Horikoshi et al., 2002), fiber optic cables (Lim et al., 2009), glass beads (Sakthivel et al., 2002), quartz sand (Choy et al., 2008), silica gel (Zainudin et al., 2010) and stainless steel (Chen & Dionysiou, 2006) were used as support materials. Inclusion of nano-photocatalyst in a polymer matrix may be an easy way for immobilization of semiconductors. But this type of polymer-nanocomposite itself is vulnerable to the degradation in presence of water, air and sunlight.

Hence semiconductor photocatalysis can also be used for degradation of plastic- semiconductor film. Polyvinyl chloride (PVC), Polyethylene (PE) and Polystyrene (PS) were among the polymeric substrates (Cho & Choi, 2001; Shang et al., 2003; Zhang et al., 2004; Fa et al., 2008; Zhao et al., 2007; Chakrabarti & Dutta, 2008) that were degraded by photocatalysis using various semiconductors.

In spite of the wide use of TiO_2 as photocatalyst, ZnO has the advantage of lower cost and absorbing larger range of solar spectrum (Sakthivel et al., 2003; Kong et al., 2009; Sil & Chakrabarti, 2010) and its efficacy also increases if

*Corresponding author. E-mail: *roy.anirban33@gmail.com*

the size is reduced in nano range. Additionally, doping with transition metals made such nanoparticles more active especially in visible region (Thongjamroon et al., 2017; Roy et al., 2016; Ahmad et al., 2013; Sher et al., 2021). There are several methods for synthesizing Fe-doped ZnO nanoparticles (Jung, 2010; Hong et al., 2007; Chen et al., 2005; Kolesnik et al., 2004; Khan et al., 2018). However in this work, we have used ultrasound assisted method because it is a green, convenient template free method (Omidi et al., 2013). A few reports are available for sonochemical synthesis and characterization of doped ZnO nanoparticles under ultrasonic irradiation (Khataee et al., 2015; Phuruangrat et al., 2014; Omidi et al., 2013) but none of them reported sonochemical synthesis of Fe-doped ZnO from an organic precursor. In a previous paper, Roy et al. (2016) reported ultrasound assisted synthesis and characterization of Fe-doped ZnO nanoparticles from a mixture of organic precursors of the two metals.

Aim of the present research was to examine whether Fe-doped ZnO semiconductor nanoparticles synthesized by Roy et al. (2016), being present in a PVC matrix, can catalyze degradation of both PVC plastic and a dye pollutant existing in the surrounding simulated wastewater under sunlight. An et al. (2014), Thomas et al. (2013) and Das et al. (2017) used nanostructured photocatalysts for degradation of polymers. But none of the above studies reported simultaneous degradation of plastics along with the pollutants present in the surrounding water.

As we know, abatement of plastic pollution is one of the major concerns of the environmentalists all over the world. In some developing countries including India waste plastics are very often thrown away into the open sewerage or water bodies and they eventually interfere with the drainage system. Human civilization has become largely dependent on plastics. Moreover in the recent pandemic situation, usage and wastage of plastics have increased by many folds (Patrício Silva et al., 2021). If a polymer composite is available which can be degraded under natural environment, it would reduce the problem of plastic pollution. It may also address simultaneously the problem of water pollution.

In this work, we have artificially created the situation of waste plastic film littered on the wastewater containing dye pollutant. The simulated waste plastic was the composite film with PVC and Fe-doped ZnO whereas the model pollutant in water was Methylene Blue dye. A few reports are available on the degradation of Methylene Blue in wastewater by semiconductor photocatalysis (Chakrabarti & Dutta, 2004; Sher et al., 2021; Khan et al., 2019) – but most of them used the catalyst in suspension. Process parameters studied for wastewater treatment were initial concentration and loading of nanoparticles. Novelty of this work was not only on the use of sunlight but also on the simultaneous degradation of solid and liquid pollutants. This has not been reported before.

1. Materials used and experimental methods

1.1. Materials

Zinc acetylacetonate [$C_{10}H_{14}O_4Zn$, denoted here as $Zn(acac)_2$ from MP Biomedicals, LLC, France] was as primary precursor; Ferric acetylacetonate [$Fe(C_5H_7O_2)_3$, denoted here as $Fe(acac)_3$ from Spectrochem Pvt. Ltd., Mumbai, India] was as dopant source; plasticizer-free PVC powder (67–01, k-value-67±1) was from Reliance Industries Limited (RIL), India; ethanol and cyclohexanone (E. Marck, Mumbai), Methylene Blue dye, C.I. No. 52015 (LOBA Chemie, Mumbai, India); single distilled water (6.8 pH, 20 μS/cm conductivity). All of the above reagents and chemicals were of analytical (AR) grade.

1.2. Experimental procedure

1.2.1. Preparation and characterization of zinc oxide nanoparticles

This has been reported in detail by Roy et al. (2016). Nanoparticles were prepared sonochemically with aqueous alcoholic solution of 0.95 mmol $Zn(acac)_2$ and 0.05 mmol $Fe(acac)_3$ in 210 ml water and 20 ml alcohol. The mixture was subjected to ultrasonication using US-probe (Trans-O-Sonic, Model: D-120/P) at 30±3 KHz frequency for 40 seconds at 1 sec pulse mode. The turbid solution was vacuum dried, washed and dried again. Characterization was executed by XRD, UV-vis spectroscopy, FESEM and EDX. XRD was done at room temperature with a diffractometer (model: X'Pert PRO, PANalytical B.V., The Netherlands) using Ni-filtered Cu Ka radiation (l = 1.5418 Å) at a scanning rate of 1 deg (2θ)/min. Generator voltage was 40 kV at current of 30 mA. The diffractogram- patterns of the nanoparticles were checked against relevant JCPDS database. Average grain sizes were calculated using Scherrer equation (Patterson, 1939).

UnitCellWin software was used to determine crystal characteristics like cell volume and lattice parameters. HITACHI U-4100 spectrophotometer was used for optical characterization. Size and surface morphology of the particles were analyzed using FESEM (JEOL-SEM/Carl Zeiss, Germany, Supra 35VP). The samples for FESEM study were prepared on glass slides. EDX analysis was done using Oxford Link Isis (UK) instrument attached to the FESEM instrument.

1.2.2. Casting and characterization of the semiconductor-PVC composite films

Fe-doped ZnO photocatalyst synthesized as before was then immobilized in a thin PVC film. The details have been described elsewhere (Das et al., 2017). A clear solution (3% w/v) was prepared by dissolving PVC powder in cyclohexanone solvent. Weighed amount of the semiconductor catalyst was added and the mixture was stirred for 8 h. The suspension was then poured on a smooth, clean glass Petri dish and the solvent was air dried at ambient condition to cast a film. Thickness of the cast film was

measured according to ASTM D 374 by using a thickness gauge (Baker, Type J17).

1.2.3. Photocatalytic degradation of dye and polymer composite film

Photocatalytic degradation under solar irradiation was carried out in a reactor fitted with a cooling water jacket and with quartz plate as the top-cover for sunlight to penetrate (Figure 1). 500 ml of Methylene blue solution of requisite concentration was taken into the reactor with PVC-Fe-ZnO film cut into pieces of small chips or flakes (approximately 1 cm^2). Oxygen was sparged with air in the reactor. Here oxygen was required as electron-scavenger. Adsorption equilibrium has been ensured after stirring the entire content in the dark for about 1 hour 15 minutes. Then the reactor and its contents were exposed to the sunlight. All the dye degradation experiments were performed under the same solar conditions during April to May. The intensity of sunlight was measured by a digital lux meter (make Dispart & Coalescent, model LX-101) was used to measure intensity of sunlight as about 52 klux (181 W/m^2). Total duration of exposure of the reaction mixture to sunlight was 2 hours 30 minutes. 5 ml aliquots samples were withdrawn at different time intervals and were analyzed by U-4100 UV-visible spectrophotometer (Hitachi, Japan) against standard calibration curve at at λ_{max} = 663 nm. Temperature of the reactor was kept approximately constant at 30 °C by cooling water circulation and pH was near neutral (6.5–7). Percent degradation was determined by using the following formula:

$$\% \text{ degradation} = \frac{\text{Initial concentration of dye} - \text{Final concentration of dye}}{\text{Initial concentration of dye}} \times 100.$$

Photocatalytic degradation of the plastic composite flakes was measured by loss in weight before and after the experiment.

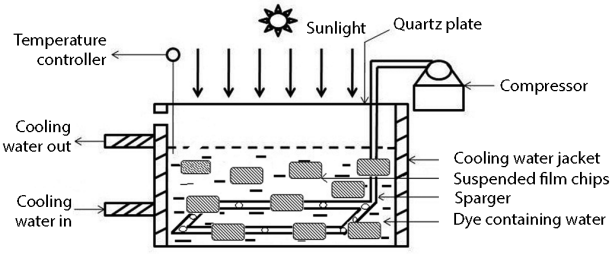

Figure 1. Schematic diagram for the experimental set up

2. Results and discussions

2.1. Characterization of the photocatalyst

Detailed characterization has been presented in our previous paper (Roy et al., 2016). A summary is given here. The X-ray diffractogram of the synthesized nanoparticles resembled JCPDS 36-1451 for standard wurtzite ZnO. 33.67 nm was the crystallite size (average) as calculated by Scherrer equation. Lattice constants found were $a = b$ = 3.23687 Å, c = 5.17894 Å. The unit cell volume was 46.9916 $(Å)^3$. An additional peak was identified at 2θ = 33.08°; this may be due to the presence of iron bearing impurity phase. The optical band gap (E_g) determined using UV-vis spectroscopy and the Tauc relation was 2.69 eV. Chakrabarti et al. (2015) reported a range of wide band gap of 2.70 to 2.80 eV for solvothermally synthesized Fe-doped ZnO. This is less than that of a pure ZnO nanoparticle. Energy required for photo-excitation is less and hence it is expected that the nanoparticles would be a better photocatalyst in visible light region (Ahmad et al., 2013; Fu et al., 2011) compared to undoped ZnO.

Figure 2 for the surface morphology of the Fe doped ZnO catalyst indicates that most of the nano-particles are like flakes. Additionally, some clustered deposits are visible on the flakes which may be due to the high surface charge. EDX result shows inclusion of iron in the ZnO crystal. Weight per cent composition of Zn, Fe and O as analyzed by EDX are 43.23, 2.79 and 53.79 respectively.

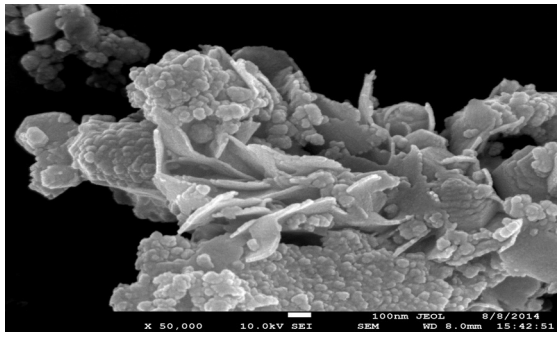

Figure 2. FESEM image of the iron-doped ZnO NPs (Roy et al., 2016)

Some important characteristics of the iron-doped nanoparticles are summarized in Table 1.

2.2. Characterization of the composite flakes

SEM analysis: Surface morphology was studied for observation of changes occurred due to degradation. Figure 3 shows the morphological changes that occurred after degradation.

Table 1. Characteristics of the Fe-doped ZnO nanoparticles

Yield %	Grain size (nm)				Lattice constants (Å)		Unit cell volume, V ($Å^3$)	Band gap energy (eV)
	Average, t	[100]	[101]	[002]	a	c		
25.90	33.67	36.36	42.94	42.72	3.23687	5.17894	46.9916	2.69

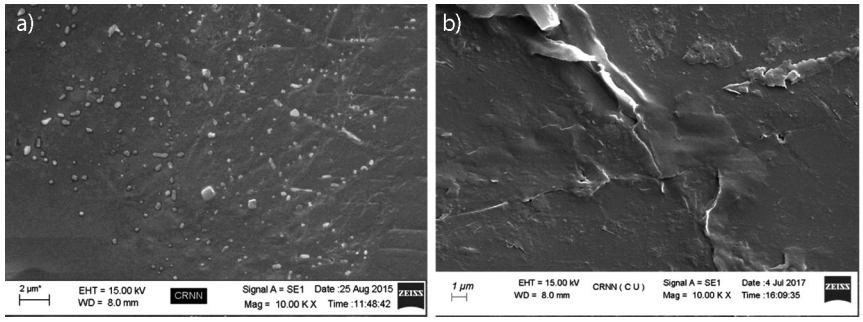

Figure 3. Surface morphology (SEM images) of PVC-Fe-ZnO nanocomposite film (a) before and (b) after degradation of dye

2.3. Proposed mechanism and kinetics

2.3.1. Photocatalytic removal of MB in solution

The steps of decolorization of dye with composite flakes are as follows:

(1) *Generation of hole-electron ($h^+ - e^-$) pair on the NP-surface embedded in the PVC matrix by the incident sunlight*

$$\mathrm{Fe-ZnO} + h\nu \rightarrow \mathrm{Fe-ZnO}\left(h^+ + e^-\right). \quad (1)$$

Sunlight had to penetrate through the polymer layer to reach the semiconductor surface. But it is difficult to quantify the resistance. Moreover a portion of the incident sunlight was utilized for direct photo degradation of the polymer.

$$\mathrm{Polymer} + h\nu \rightarrow \mathrm{Polymer}\bullet. \quad (2)$$

(2) *Generation of free* •OH *radical as well as on the catalyst surface*

$$\mathrm{Fe-ZnO}\left(e^-\right) + \frac{1}{2}O_2 + H_2O \rightarrow \mathrm{Fe-ZnO} + OH^- + \bullet OH; \quad (3)$$

$$\mathrm{Fe-ZnO}\left(h^+\right) + H_2O \rightarrow \mathrm{Fe-ZnO}\ldots\bullet OH + H^+. \quad (4)$$

(3) *Diffusion of dye molecule from the bulk to the surface of the composite film*

Since the reaction mixture is well agitated, this diffusion is expected to be fast and hence mass transfer resistance would be negligible.

(4) *Adsorption of dye molecule on the composite flake surface*

Adsorption is pre-requisite for a catalytic process. For studying this adsorption, data of the dark reaction with different initial concentrations are used. It was observed that the equilibrium data fitted well to the Langmuir isotherm equation (Figure 4).

$$q_e = \frac{q_m K_L C_e}{1 + K_L C_e}, \quad (5)$$

where q_e – dye adsorbed in mg/g, q_m – maximum adsorption capacity (Langmuir) in mg/g, C_e – concentration of the solution in mg/L at equilibrium, K_L – Langmuir constant in L/mg.

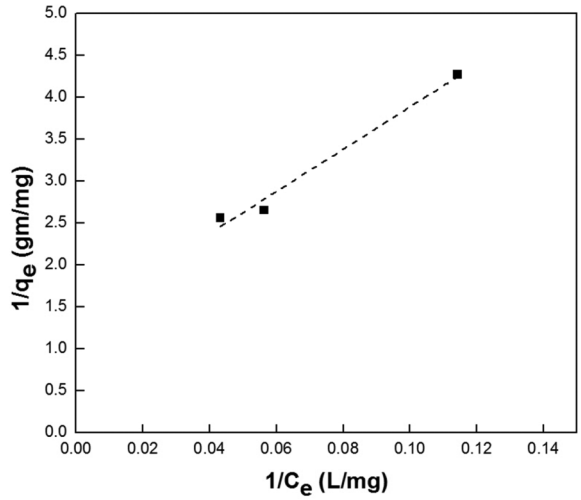

Figure 4. Fitting of dark reaction data in Langmuir adsorption isotherm equation

Using the above form of Langmuir equation, the values of the constants of Eq. (5) were determined. q_m and K_L calculated from slope and intercept of the straight-line plot (R^2 = 0.983) were 0.733138 mg/g and 0.54084 L/mg respectively. Chakrabarti and Dutta (2004) observed a Langmuir constant of 8.62×10^{-3} L/mg for a bulk ZnO-Methylene Blue system.

For studying the rate of adsorption of the dye onto the polymer composite flakes, the time-concentration data from the dark reaction were fitted with the well-known Lagergren pseudo first order equation.

$$\log\left(q_e - q_t\right) = \log q_e - kt, \quad (6)$$

where q_e and q_t are the concentration of dye on solid adsorbent (mg/g) at equilibrium and at any time, t (min), respectively, and k is the rate constant of Lagergren pseudo-first-order sorption (L/min).

Plots of the LHS of Eq. (6) against time with different initial concentrations are given in Figure 5. Rate constants with different initial concentrations as well as with different NP-loading are given in Table 2. It shows decrease in the value of rate constant decrease with increase in the initial substrate concentration for the presence of more substrate molecules than the active sites can accommodate. Up to a certain extent, rate of adsorption increased with

increase in nanoparticle-loading into the polymer matrix. After that critical value, the rate decreased with increase in loading because of the "crowd" so that the surface was not available for adsorption.

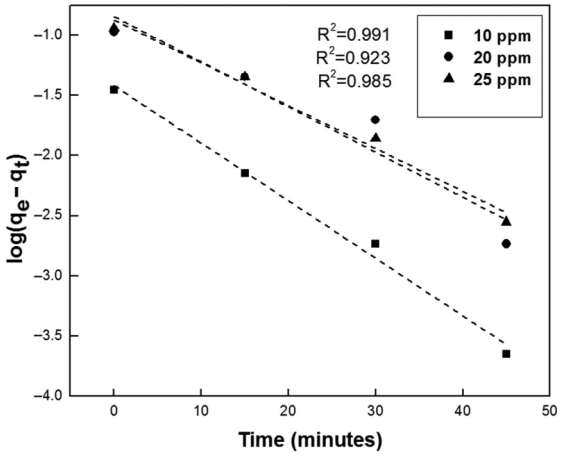

Figure 5. $\log(q_e - q_t)$ against time plot at different initial concentrations

Table 2. Lagergren pseudo- first order rate constants for adsorption of MB dye on PVC-Fe-ZnO nanocomposite

Initial concentration, mg/L	k (min^{-1})	R^2	NP loading, (g/g of PVC)	k (min^{-1})	R^2
10	0.04786	0.991	0.033	0.04786	0.991
20	0.03753	0.923	0.067	0.06207	0.966
25	0.03559	0.985	0.1	0.03054	0.946

(5) *Diffusion of MB dye molecules through the polymer matrix to the semiconductor surface*

Since the loading of NPs in the composite film is small (0.1% w/v) the resistance due to step (5) cannot be neglected. Diffusion through solid polymer matrix is a slow process. Since doping decreases the band gap, there may also be a competition between recombination of hole -electron pair with the diffusion of dye through polymer matrix. No attempt has been made in this report to quantify this phenomenon separately.

(6) *Adsorption of the dye molecules on the nanoparticle surface*

In step (4) above, adsorption of dye on the surface of the composite film has been described. But it is not easy to distinguish between adsorption on the polymer surface and adsorption on the nanoparticle surface. Hence adsorption on the composite as a whole is considered.

(7) *Reaction of the dye molecule with the free and surface-bound* •OH *radical*

$$\text{Dye} + \bullet\text{OH} \rightarrow \text{Products}; \quad (7)$$

$$\text{Dye} + \text{Fe}-\text{ZnO}\ldots\bullet\text{OH} \rightarrow \text{Products} + \text{Fe}-\text{ZnO} + \text{H}_2\text{O}. \quad (8)$$

In this stage also there will be a competition between the degradation of dye and polymer matrix with the available •OH radicals.

For the sake of simplified quantitative description of the phenomenon of dye removal, the decolorization has been lumped into two phases – removal of dye by adsorption on the composite film (dark) and the removal of dye by photocatalytic process (light) after adsorption equilibrium is reached. The trend is demonstrated in Figure 6. Accordingly the time-concentration (kinetic) data have been fitted into two stages – the first one for adsorption by Lagergren pseudo first order equation and the second one for photocatalysis with Langmuir-Hinshelwood equation.

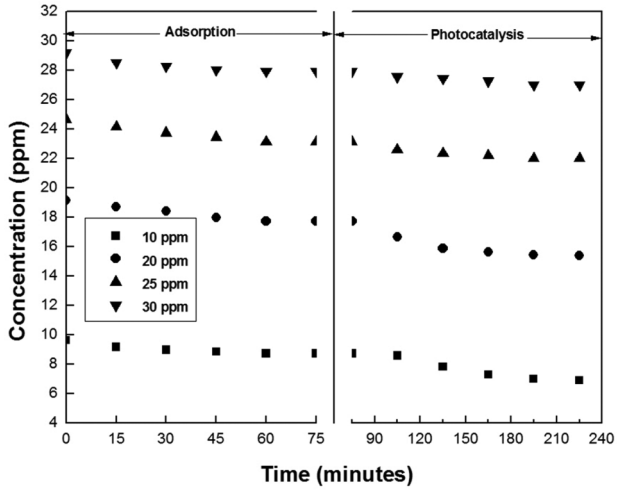

Figure 6. Two stage time-concentration profiles of dark and photo reactions with varying initial concentration of dye

The well-known Langmuir-Hinshelwood equation for heterogeneous catalysis modified to explain reaction at the solid-liquid interface is as follows (Poulios & Tsachpinis, 1999; Chakrabarti & Dutta, 2004):

$$r_0 = -\frac{dc}{dt} = \frac{k_r K C_e}{1 + K C_e}, \quad (9)$$

where r_0 – initial rate of reaction in mg/l min, k_r – rate constant for photocatalys is in mg/l min, K – rate constant for adsorption in l/mg, C_e – equilibrium concentration of bulk solution in ppm or mg/l, C – concentration of bulk solution at any time t (minutes).

The term KC_e is often negligible as low concentration, and the reaction rate can be expressed on the basis of a pseudo-first order model. So the modified model can be represented as:

$$-\frac{dC}{dt} = k_r K C_e = K_{app} C_e, \quad (10)$$

where K_{app} – apparent first order reaction rate constant. Integrating Eq. (10) yields Eq. (11):

$$\ln\left(\frac{C}{C_e}\right) = -K_{app} t. \quad (11)$$

Slope of the plot of $-\ln(C/C_e)$ against t yields the value of the lumped rate constant K_{app} (Table 3). It indicates that photocatalytic degradation of dye at the reactions

conditions follows a pseudo-first-order kinetic equation. This result corroborates the same by other researchers (Hosseini et al., 2007; Royaee & Sohrabi, 2010).

Table 3. First order (apparent) rate constants for photocatalytic degradation of Methylene Blue

Initial concentration	K_{app} (min^{-1})	R^2	NP loading (g/g of PVC)	K_{app} (min^{-1})	R^2
10	0.00170	0.950	0.033	0.00174	0.950
20	0.00117	0.743	0.067	0.00193	0.852
25	0.00040	0.794	0.1	0.00155	0.848
30	0.00026	0.932	0.133	0.00143	0.732

2.3.2. Degradation of the polymer nanocomposite flakes

A net decrease in weight of the flakes from 0.7823 g to 0.7429 g after reaction supports this proposition. In fact, herein lies the novelty of the process – it degrades both dye and polymer with the help of sunlight. As the flakes were small and many in numbers and were difficult to collect, dry and weigh intermittently, time- weight loss profile could not be constructed like that were made before (Chakrabarti et al., 2008; Sil & Chakrabarti, 2010; Das et al., 2017). In our previous work, the weight –loss of the film also followed pseudo-first order kinetics.

Mechanism and kinetic model of solar photo-degradation of PVC-Fe-ZnO composite film has been described elsewhere (Sil & Chakrabarti 2010; Das et al., 2017). A summary is presented as below:

$$\text{Polymer} + \text{Fe} - \text{ZnO}\ldots\bullet\text{OH} \rightarrow \text{Polymer}\bullet + \text{Fe} - \text{ZnO} + \text{H}_2\text{O}; \quad (12)$$

$$\text{Polymer} + \bullet\text{OH} \rightarrow \text{Polymer}\bullet + \text{H}_2\text{O}. \quad (13)$$

Overall degradation rate constant was dependent on the rate of photo excitation of semiconductor by Eq. (1) and the rate of photolysis by Eq. (2). The former had a relationship with the amount or loading of the photocatalyst. Mathematically,

$$k' = 2k_1\left[\text{Fe} - \text{ZnO}\right] + k_6, \quad (14)$$

where $k' = \dfrac{k}{\dfrac{I_f}{\rho l}}$.

A plot of nano photocatalyst loading [Fe-ZnO] against the pseudo first order rate constants *k'* at various catalyst-loading yielded k_1 (rate constant for the photo excitation of semiconductor) and k_6 (rate of photolysis). I_f was intensity of light (W/m^2), ρ was density of polymer (kg/m^3) and *l* was thickness of the film (m).

2.4. Influence of process parameters

Solar photocatalytic degradation of MB dye are influenced by the initial dye concentration and loading of NPs in the PVC matrix at the constant intensity of sunlight. Initial concentrations were varied from 10–30 mg/L. Here the loading of nanoparticle was fixed at 0.033 (g/g of PVC). As expected, the concentration of MB as well as the rate constant decreased with increasing concentration. As the initial concentration was increased from 10 to 30 mg/L, percent degradation decreased from 28.06 to 7.58% in about 4 h. As previously explained, total degradation includes removal by adsorption as well.

Experiments were also conducted by varying the amount of nano catalyst loading in polymer from 0.033–0.133 (g/g of PVC) keeping initial concentration of dye at 10 mg/L. Maximum percent decolorization (28.21) and rate was obtained at the loading of 0.067 g/g PVC. Blank experiment with pure PVC film showed no degradation of dye pollutant.

However demineralization of dye was not much as indicated by negligible change in the COD (chemical oxygen demand) value of the dye solution before and after the reaction. It may be due to generation of colourless oxidizable intermediates and products both from the dye and from the composite film.

2.5. Solar photo (catalytic) – degradation of the solid plastic flakes

Under the condition of maximum degradation of dye pollutant (28%), 5% of the initial weight of the PVC-composite film was reduced after 3 hours 45 minutes. Hence 28% of liquid phase pollutant was degraded at the cost of 5% degradation of plastic pollutant.

Conclusions

A novel process of simultaneous solar photocatalytic degradation of MB dye in water and PVC-Fe-ZnO under sunlight has been examined. A composite film was made by immobilizing sonochemically synthesized Fe-doped ZnO nanoparticles dispersed in PVC matrix. The nanoparticles were characterized by XRD, FESEM and UV-vis spectrophotometry. SEM was used for surface morphology of the film before and after degradation. Solar photocatalytic degradation of the polymer composite film as well as of the MB dye dissolved in the surrounding water was studied. The nanocomposite film was found to be self-destructive. Process parameters influencing the degradation were initial concentration of dye and loading of the Fe-doped ZnO catalyst. MB dye in water was degraded under sunlight alongwith degradation of the film itself. Within 3 h 45 minutes the maximum decolorization was 28%. The loss in weight of the film was 5.04%. Both adsorption and photocatalytic decolorization separately followed pseudo first order rate equation. Mechanism for the degradation was discussed. Immobilized nanoparticles in polymer matrix decreased the post-treatment separation cost.

Acknowledgements

TEQIP, phase-II, University of Calcutta for fellowship to A. Roy, Prof. Binay Kanti Dutta for advice, Dr. Paramita Das for suggestion regarding PVC film formation; Prof. Dipankar Chattopadhyay (Dept. of PST, University of Calcutta) for XRD; Dr. Prantik Banerjee (West Bengal Pollution Control Board, WBPCB, now in Adamas University) for suggestion during nano-particle synthesis and characterization; CRNN-CU for SEM-EDX and FESEM.

References

Ahmad, M., Ahmed, E., Hong, Z. L., Jiao, X. L., Abbas, T., & Khalid, N. R. (2013). Enhancement in visible light-responsive photocatalytic activity by embedding Cu-doped ZnO nanoparticles on multi-walled carbon nanotubes. *Applied Surface Science*, *285*(Part B), 702–712. https://doi.org/10.1016/j.apsusc.2013.08.114

Ai, Z. H., Huang, Y. H., Lee, S. C., & Zhang, L. Z. (2011). Monoclinic Bi_2O_3 photocatalyst for efficient removal of gaseous NO and HCHO under visible light irradiation. *Journal of Alloys and Compounds*, *509*(5), 2044–2049. https://doi.org/10.1016/j.jallcom.2010.10.132

An, Y., Hou, J., Liu, Z., & Peng, B. (2014). Enhanced solid-phase photocatalytic degradation by TiO_2-MWCNTs nanocomposites. *Materials Chemistry and Physics*, *148*(1–2), 387–394. https://doi.org/10.1016/j.matchemphys.2014.08.001

Chakrabarti, S., & Dutta, B. K. (2004). Photocatalytic degradation of model textile dyes in wastewater using ZnO as semiconductor catalyst. *Journal of Hazardous Materials*, *112*(3), 269–278. https://doi.org/10.1016/j.jhazmat.2004.05.013

Chakrabarti, S., & Dutta, B. K. (2008). Dye-sensitised photocatalytic degradation of PVC-ZnO composite film. *International Journal of Environmental Technology and Management*, *9*(1), 34–46. https://doi.org/10.1504/IJETM.2008.017858

Chakrabarti, S., Chaudhuri, B., Bhattacharjee, S., Das, P., & Dutta, B. K. (2008). Degradation mechanism and kinetic model for photocatalytic oxidation of PVC–ZnO composite film in presence of a sensitizing dye and UV radiation. *Journal of Hazardous Materials*, *154*(1–3), 230–236. https://doi.org/10.1016/j.jhazmat.2007.10.015

Chakrabarti, S., Liu, X., Li, C., Banerjee, P., Maitra, S., & Swihart, M. T. (2015). Synthesis of iron-doped zinc oxide nanoparticles by simple heating: Influence of precursor composition and temperature. *International Journal of Materials Engineering Innovation*, *6*(1), 18–31. https://doi.org/10.1504/IJMATEI.2015.069798

Chen, Y. W., Liu, Y. C., Lu, S. X., Xu, C. S., Shao, C. L., Wang, C., Zhang, J. Y., Lu, Y. M., Shen, D. Z., & Fan, X. W. (2005). Optical properties of ZnO and ZnO: Al in nanorods assembled by sol-gel method. *The Journal of Chemical Physics*, *123*(13), 134701–134705. https://doi.org/10.1063/1.2009731

Chen, Y., & Dionysiou, D. D. (2006). TiO_2 photocatalytic films on stainless steel: The role of Degussa P-25 in modified sol–gel methods. *Applied Catalysis B: Environmental*, *62*(3–4), 255–264. https://doi.org/10.1016/j.apcatb.2005.07.017

Cho, S., & Choi, W. (2001). Solid-phase photocatalytic degradation of PVC–TiO_2 polymer composites. *Journal of Photochemistry and Photobiology A: Chemistry*, *143*(2–3), 221–228. https://doi.org/10.1016/S1010-6030(01)00499-3

Chong, M. N., Jin, B., Chow, C. W. K., & Saint, C. (2010). Recent developments in photocatalytic water treatment technology: A review. *Water Research*, *44*(10), 2997–3027. https://doi.org/10.1016/j.watres.2010.02.039

Choy, C. C., Wazne, M., & Meng, X. (2008). Application of an empirical transport model to simulate retention of nanocrystalline titanium dioxide in sand columns. *Chemosphere*, *67*(9), 1794–1801. https://doi.org/10.1016/j.chemosphere.2007.12.030

Das, P., Roy, A., & Chakrabarti, S. (2017). Photocatalytic degradation of the nanocomposite film comprising polyvinyl chloride (PVC) and sonochemically synthesized iron-doped zinc oxide: A comparative study of performances between sunlight and UV radiation. *Journal of Polymers and the Environment*, *25*(4), 1231–1241. https://doi.org/10.1007/s10924-016-0894-0

Fa, W., Zan, L., Gong, C., Zhong, J., & Deng, K. (2008). Solid-phase photocatalytic degradation of polystyrene with TiO_2 modified by iron (II) phthalocyanine. *Applied Catalysis B: Environmental*, *79*(3), 216–223. https://doi.org/10.1016/j.apcatb.2007.10.018

Fu, M., Li, Y., Wu, S., Lu, P., Liu, J., & Dong, F. (2011). Sol–gel preparation and enhanced photocatalytic performance of Cu-doped ZnO nanoparticles. *Applied Surface Science*, *258*(4), 1587–1591. https://doi.org/10.1016/j.apsusc.2011.10.003

Hong, N. H., Sakai, J., & Briz, V. (2007). Observation of ferromagnetism at room temperature in ZnO thin films. *Journal of Physics: Condensed Matter*, *19*(3), 036219. https://doi.org/10.1088/0953-8984/19/3/036219

Horikoshi, S., Watanabe, N., Onishi, H., Hidaka, H., & Serpone, N. (2002). Photodecomposition of a nonylphenol polyethoxylate surfactant in a cylindrical photoreactor with TiO_2 immobilized fiber glass cloth. *Applied Catalysis B: Environmental*, *37*(2), 117–129. https://doi.org/10.1016/S0926-3373(01)00330-7

Hosseini, S. N., Borghei, S. M., Vossough, M., & Taghavinia, N. (2007). Immobilization of TiO_2 on perlite granules for photocatalytic degradation of phenol. *Applied Catalysis B: Environmental*, *74*, 53–62. https://doi.org/10.1016/j.apcatb.2006.12.015

Jung, D. (2010). Syntheses and characterization of transition metal-doped ZnO. *Solid State Sciences*, *12*(4), 466–470. https://doi.org/10.1016/j.solidstatesciences.2009.12.009

Khan, S. A., Arshad, Z., Shahid, S., Arshad, I., Rizwan, K., Sher, M., & Fatima, U. (2019). Synthesis of TiO_2/Graphene oxide nanocomposites for their enhanced photocatalytic activity against methylene blue dye and ciprofloxacin. *Composites Part B: Engineering*, *175*, 107120. https://doi.org/10.1016/j.compositesb.2019.107120

Khan, S. A., Noreen, F., Kanwal, S., Iqbal, A., & Hussain, G. (2018). Green synthesis of ZnO and Cu-doped ZnO nanoparticles from leaf extracts of *Abutilon indicum*, *Clerodendrum infortunatum*, *Clerodendrum inerme* and investigation of their biological and photocatalytic activities. *Materials Science and Engineering: C*, *82*, 46–59. https://doi.org/10.1016/j.msec.2017.08.071

Khataee, A., Soltani, R. D. C., Karimi, A., & Joo, S. W. (2015). Sonocatalytic degradation of a textile dye over Gd-doped ZnO nanoparticles synthesized through sonochemical process. *Ultrasonics Sonochemistry*, *23*, 219–230. https://doi.org/10.1016/j.ultsonch.2014.08.023

Kolesnik, S., Dabrowski, B., & Mais, J. (2004). Structural and magnetic properties of transition metal substituted ZnO. *Journal of Applied Physics*, *95*(5), 2582–2586. https://doi.org/10.1063/1.1644638

Kong, J. Z., Li, A. D., Zhai, H. F., Gong, Y. P., Li, H., & Wu, D. (2009). Preparation, characterization of the Ta-doped ZnO

nanoparticles and their photocatalytic activity under visible-light illumination. *Journal of Solid State Chemistry*, *182*(8), 2061–2067. https://doi.org/10.1016/j.jssc.2009.03.022

Lim, L. L. P., Lynch, R. J., & In, S.-I. (2009). Comparison of simple and economical photocatalyst immobilisation procedures. *Applied Catalysis A: General*, *365*(2), 214–221. https://doi.org/10.1016/j.apcata.2009.06.015

Omidi, A., Habibi-Yangjeh, A., & Pirhashemi, M. (2013). Application of ultrasonic irradiation method for preparation of ZnO nanostructures doped with Sb^{+3} ions as a highly efficient photocatalyst. *Applied Surface Science*, *276*(1), 468–475. https://doi.org/10.1016/j.apsusc.2013.03.118

Patrício Silva, A. L., Prata, J. C., Walker, T. R., Duarte, A. C., Ouyang, W., Barcelò, D., & Rocha-Santos, T. (2021). Increased plastic pollution due to COVID-19 pandemic: Challenges and recommendations. *Chemical Engineering Journal*, *405*, 126683. https://doi.org/10.1016/j.cej.2020.126683

Patterson, A. L. (1939). The Scherrer formula for X-ray particle size determination. *Physical Review*, *56*(10), 978–982. https://doi.org/10.1103/PhysRev.56.978

Phuruangrat, A., Yayapao, O. Thongtem, T., & Thongtem, S. (2014). Preparation, characterization and photocatalytic properties of Ho doped ZnO nanostructures synthesized by sonochemical method. *Superlattices and Microstructures*, *67*, 118–126. https://doi.org/10.1016/j.spmi.2013.12.023

Poulios, I., & Tsachpinis, I. (1999). Photodegradation of the textile dye Reactive Black 5 in the presence of semiconducting oxides. *Journal of Chemical Technology and Biotechnology*, *74*(4), 349–357. https://doi.org/10.1002/(SICI)1097-4660(199904)74:4<349::AID-JCTB5>3.0.CO;2-7

Roy, A., Maitra, S., Ghosh, S., & Chakrabarti, S. (2016). Sonochemically synthesized iron-doped zinc oxide nanoparticles: influence of precursor composition on characteristics. *Materials Research Bulletin*, *74*, 414–420. https://doi.org/10.1016/j.materresbull.2015.11.006

Royaee, S. J., & Sohrabi, M. (2010). Application of photo-impinging streams reactor indegradation of phenol in aqueous phase. *Desalination*, *253*, 57–61. https://doi.org/10.1016/j.desal.2009.11.033

Sakthivel, S., Neppolian, B., Shankar, M. V., Arabindoo, B., Palanichamy, M., & Murugesan, V. (2003). Solar photocatalytic degradation of azo dye: comparison of photocatalytic efficiency of ZnO and TiO_2. *Solar Energy Materials and Solar Cells*, *77*(1), 65–82. https://doi.org/10.1016/S0927-0248(02)00255-6

Sakthivel, S., Shankar, M. V., Palanichamy, M., Arabindoo, B., & Murugesan, V. (2002). Photocatalytic decomposition of leather dye: comparative study of TiO_2 supported on alumina and glass beads. *Journal of Photochemistry and Photobiology A: Chemistry*, *148*(1–3), 153–159. https://doi.org/10.1016/S1010-6030(02)00085-0

Shang, J., Chai, M., & Zhu, Y. (2003). Photocatalytic degradation of polystyrene plastic under fluorescent light. *Environmental Science & Technology*, *37*(19), 4494–4499. https://doi.org/10.1021/es0209464

Sher, M., Khan, S. A., Shahid, S., Javed, M., Qamar, M. A., Chinnathambi, A., & Almoallim, H. S. (2021). Synthesis of novel ternary hybrid g-C3N4@Ag-ZnO nanocomposite with Z-scheme enhanced solar light-driven methylene blue degradation and antibacterial activities. *Journal of Environmental Chemical Engineering*, *9*(4), 105366. https://doi.org/10.1016/j.jece.2021.105366

Shi, J., Zheng, J., Wu, P., & Ji, X. (2008). Immobilization of TiO_2 films on activated carbon fiber and their photocatalytic degradation properties for dye compounds with different molecular size. *Catalysis Communications*, *9*(9), 1846–1850. https://doi.org/10.1016/j.catcom.2008.02.018

Sil, D., & Chakrabarti, S. (2010). Photocatalytic degradation of PVC-ZnO composite film under tropical sunlight and artificial UV radiation: A comparative study. *Solar Energy*, *84*(3), 476–485. https://doi.org/10.1016/j.solener.2009.09.012

Thomas, R. T., Nair, V., & Sandhyarani, N. (2013). TiO_2 nanoparticle assisted solid phase photocatalytic degradation of polythene film: A mechanistic investigation. *Colloids and Surfaces A: Physicochemical and Engineering Aspects*, *422*, 1–9. https://doi.org/10.1016/j.colsurfa.2013.01.017

Thongjamroon, S., Ding, J., Herng, T. S., Tang, I. M., & Thongmee, S. (2017). Dependence of the magnetic properties of the dilute magnetic semiconductor $Zn_{1-x}Mn_xO$ nanorods on their Mn doping levels. *Journal of Magnetism and Magnetic Materials*, *439*, 391–396. https://doi.org/10.1016/j.jmmm.2017.04.087

Wang, X., Yao, S., & Li, X. (2009). Sol-gel preparation of CNT/ZnO nanocomposite and its photocatalytic property. *Chinese Journal of Chemistry*, *27*(7), 1317–1320. https://doi.org/10.1002/cjoc.200990220

Zainudin, N. F., Abdullah, A. Z., & Mohamed, A. R. (2010). Characteristics of supported nano-TiO_2/ZSM-5/silica gel (SNTZS): Photocatalytic degradation of phenol. *Journal of Hazardous Materials*, *174*(1–3), 299–306. https://doi.org/10.1016/j.jhazmat.2009.09.051

Zhang, K., Cao, W., & Zhang, J. (2004). Solid-phase photocatalytic degradation of PVC by Tungstophosphoric acid—a novel method for PVC plastic degradation. *Applied Catalysis A: General*, *276*(1–2), 67–73. https://doi.org/10.1016/j.apcata.2004.07.056

Zhao, X., Li, Z., Chen, Y., Shi, L., & Zhu, Y. (2007). Solid-phase photocatalytic degradation of polyethylene plastic under UV and solar light irradiation. *Journal of Molecular Catalysis A: Chemical*, *268*(1–2), 101–106. https://doi.org/10.1016/j.molcata.2006.12.012